

# Factors Affecting $^{131}\text{I}$ -Lym-1 Pharmacokinetics and Radiation Dosimetry in Patients with Non-Hodgkin's Lymphoma and Chronic Lymphocytic Leukemia

Gerald L. DeNardo, Sally J. DeNardo, Sui Shen, Diane A. DeNardo, Gary R. Mirick, Daniel J. Macey and Kathleen R. Lamborn

University of California Davis Medical Center, Sacramento; University of California San Francisco, San Francisco, California; and University of Alabama, Birmingham, Alabama

Lym-1, a monoclonal antibody that preferentially targets malignant lymphocytes, has induced therapeutic responses in patients with non-Hodgkin's lymphoma (NHL) and chronic lymphocytic leukemia (CLL) when labeled with  $^{131}\text{I}$ . Responders had statistically significant prolongation of survival compared with nonresponders. The nonmyeloablative, maximum tolerated dose for each of two doses of  $^{131}\text{I}$ -Lym-1 was 3.7 GBq/m<sup>2</sup> (total 7.4 GBq/m<sup>2</sup> [100 mCi/m<sup>2</sup>, total 200 mCi/m<sup>2</sup>]) of body surface area. The purpose of this study was to determine the pharmacokinetics and radiation dosimetry for the initial  $^{131}\text{I}$ -Lym-1 therapy dose in patients with NHL and CLL and to compare tumor dosimetry with  $^{131}\text{I}$ -Lym-1 dosing and other patient parameters. **Methods:** Fifty-one patients with stage 3 or 4 lymphoma were treated with  $^{131}\text{I}$ -Lym-1 (0.74–8.04 GBq [20–217 mCi]) in either a maximum tolerated dose (MTD) or low-dose (LD) trial. Total Lym-1 given to each patient was sufficient in all instances to exceed the threshold required for stable pharmacokinetics. Quantitative imaging and physical examination, including caliper and CT measurement of tumor size and analysis of blood, urine and feces, were performed for a period of 7 to 10 d after infusion to assess pharmacokinetics and radiation dosimetry. Clinical records were reviewed to obtain data required for comparative assessments. **Results:** The concentration (%ID/g) and biologic half-time of  $^{131}\text{I}$ -Lym-1 in tumor were about twice those in normal tissues, although tumor half-time was similar to that of the thyroid. Pharmacokinetics were similar for patients in the MTD and LD trials, and for NHL and CLL patients in the LD trial, except that the latter group had less tumor concentration of  $^{131}\text{I}$ . Mean tumor radiation dose per unit of administered  $^{131}\text{I}$  was 1.0 Gy/GBq (3.7 rad/mCi) for patients with NHL whether in MTD or LD trials, about nine times greater than that for body or marrow. Tumor radiation dose was less and liver radiation dose was more in patients with CLL. Otherwise, radiation dosimetry was, on average, remarkably similar among groups of patients and among individual patients. Pharmacokinetics and dosimetry did not appear to be influenced by the amount of  $^{131}\text{I}$  or Lym-1 within the ranges administered. Tumor concentration of  $^{131}\text{I}$  and radia-

tion dose per gigabecquerel were inversely related to tumor size but did not seem to be related to histologic grade or type, tumor burden or therapeutic response. **Conclusion:** The therapeutic index of  $^{131}\text{I}$ -Lym-1 was favorable, although the index for patients with CLL was less than that for patients with NHL. Pharmacokinetics and radiation dosimetry were, on average, remarkably similar among patients and groups of patients in different trials.

**Key Words:** antibody; radioimmunotherapy;  $^{131}\text{I}$ ; dosimetry; cancer

**J Nucl Med 1999; 40:1317–1326**

**A**lthough combination chemotherapy and external beam radiotherapy are effective in early disease and for palliation of late disease, most patients with non-Hodgkin's lymphoma (NHL) and chronic lymphocytic leukemia (CLL) fail to achieve long-term, disease-free survival (1). The high mortality rate is especially significant, because the rate of occurrence of NHL has increased substantially in recent decades (2). The potential of radioimmunotherapy (RIT) in lymphoma was first demonstrated when a patient with Richter's lymphomatous transformation of CLL was treated effectively using  $^{131}\text{I}$ -Lym-1 (3). Since then, many reports have verified the potential of radiolabeled antibodies for treatment of NHL (4–9) and other hematological malignancies (10–12).  $^{131}\text{I}$  has been the primary radionuclide used for RIT, because it is inexpensive, widely available and readily incorporated into proteins.

Lym-1 is a monoclonal antibody that preferentially targets malignant lymphocytes and has been shown to induce therapeutic responses in most patients with NHL and CLL (4,9,13,14). Because of these promising results, the purpose of this study was to examine the pharmacokinetics and radiation dosimetry for the initial therapy dose of  $^{131}\text{I}$ -Lym-1 given to 51 adult patients, 46 with NHL and 5 with CLL. The effects on pharmacokinetics and radiation dosimetry of the type of malignancy, NHL versus CLL, and the treatment trial

Received Aug. 7, 1998; revision accepted Feb. 4, 1999.

For correspondence or reprints contact: Gerald L. DeNardo, MD, Molecular Cancer Institute, 1508 Alhambra Blvd., Rm. 3100, Sacramento, CA 95816.

(4,9), maximum tolerated dose (MTD) (1.5–3.7 GBq [40–100 mCi]) per square meter of body surface area versus low dose (LD) (1.1 or 2.2 GBq [30 or 60 mCi]) total dose, were assessed. Additionally, tumor concentration of  $^{131}\text{I}$  and radiation dose were compared with the following: Lym-1 (mg),  $^{131}\text{I}$  dose (GBq), tumor size (g), histologic grade and type, therapeutic response and tumor burden as reflected by serum lactic dehydrogenase (LDH). Each patient received an amount of Lym-1 previously shown to be sufficient to block nonspecific binding sites and to provide stable pharmacokinetics.

## MATERIALS AND METHODS

### Patients

Fifty-one patients (32 men, 19 women; median age 57 y, range 29–74 y) entered trials using  $^{131}\text{I}$ -Lym-1 therapy, providing data for this analysis. Forty-six patients had NHL and 5 had CLL; 47 patients had Ann Arbor stage 4 NHL, and 4 patients had Ann Arbor stage 3 NHL. Nine patients had high-grade, 26 had intermediate-grade and 16 had low-grade histologies when CLL was regarded as low grade. Twenty-one patients had marrow involvement, and 42 had extranodal disease. Splenectomy had been done on 6 patients, 3 NHL and 3 CLL patients. Before treatment, all but 1 patient had tumor tissue that was reactive to Lym-1 antibody; the pharmacokinetics and dosimetry for the Lym-1 negative patient were similar to those of the other patients, although tumor was not identified. All patients had serum that tested negative for human anti-mouse antibody (HAMA) and had received no cancer therapy for at least 4 wk. NHL histologic grade and type were determined in accordance with the working formulation (15); CLL was classified as low grade. Before treatment, all patients were advised of the investigational nature of the trial and signed an informed consent for protocols that were approved by the University of California at Davis Human Subjects and Radiation Use Committees under an investigational new drug authorization from the U.S. Food and Drug Administration. Patients were entered in either of two trials. For one trial, individual  $^{131}\text{I}$ -Lym-1 doses were escalated in patient cohorts to determine the MTD per square meter of body surface area. For the other trial, individual doses of 1.1 or 2.2 GBq (30 or 60 mCi) total were given. Although most patients received multiple doses on either the MTD (1.5–3.7 GBq/m<sup>2</sup> [40–100 mCi/m<sup>2</sup>]) or the LD (1.1 or 2.2 GBq, 0.5–1.5 GBq/m<sup>2</sup> [30 or 60 mCi, 14–40 mCi/m<sup>2</sup>]) trial, only results for the first therapy doses are reported here. Dosimetry for the first therapy dose was selected because it has been observed to be similar to that for the corresponding imaging dose (14,16) and subsequent therapy doses (G. DeNardo, unpublished data) but is more reliable because of high signal  $^{131}\text{I}$  imaging and temporally related radiographs. The mean administered  $^{131}\text{I}$  was 5.26 GBq (range 3.41–8.04 GBq [142 mCi, range 92–217 mCi]) for MTD patients and 1.55 GBq (range 0.74–2.56 GBq [42 mCi, range 20–69 mCi]) for LD patients. Pharmacokinetics and radiation dosimetry were determined for total body, liver, spleen, blood, marrow and tumor in all 51 patients and for lung, kidney and thyroid in a subgroup of 30 patients.

### Radiopharmaceutical

Lym-1 is an IgG2a mouse monoclonal antibody with high affinity against a discontinuous epitope on the beta subunit of the human leukocyte antigen-DR antigen located on the surface membrane of malignant B-lymphocytes (17,18). The hybridoma

was generated by fusion of splenic lymphocytes of mice that were immunized with nuclei from Raji cells that originated from a patient with Burkitt's lymphoma. Lym-1 was either produced in our laboratory from BALB/c mouse ascitic fluid and purified by ammonium sulfate precipitation and protein A-Sepharose affinity chromatography or was obtained from Damon Biotech, Inc. (Needham Heights, MA) or Techniclone, Inc. (Tustin, CA) and prepared according to specifications. Radioiodination was achieved using chloramine-T and high specific activity  $^{131}\text{I}$  sodium iodide in 0.05 N sodium hydroxide. The  $^{131}\text{I}$ -Lym-1 radiopharmaceutical contained approximately 370 MBq (10 mCi)  $^{131}\text{I}$  per milligram of Lym-1. Cellulose acetate electrophoresis and high-performance liquid chromatography showed that at least 90% of  $^{131}\text{I}$ -Lym-1 behaved like an immunoglobulin of 150 kDa. Immunoreactivity of  $^{131}\text{I}$ -Lym-1 was at least 87% of that of unmodified Lym-1. All radiopharmaceutical products were documented to be pyrogen free.

Before infusion of  $^{131}\text{I}$ -Lym-1, and on at least 4 subsequent days, 0.5–1 mL Lugol's solution (500 mg/mL) or a saturated solution of potassium iodide (830 mg/mL) was administered orally to block thyroid uptake of released  $^{131}\text{I}$ . Unlabeled Lym-1 (preload) was given intravenously in different amounts before infusion of  $^{131}\text{I}$ -Lym-1 to determine the optimum biologic dose; there were no differences in the pharmacokinetics of  $^{131}\text{I}$ -Lym-1 for preload doses  $\geq 5$  mg.

### Data Collection

Acquisition methods for transmission and emission images have been previously described (19). Briefly, transmission images in the presence and absence of the patient were acquired using an  $^{131}\text{I}$  rod source to determine attenuation factors for correction of specific tissues. Serial planar imaging data were collected on an Orbiter 7500 or Bodyscan camera (Siemens Medical Systems, Inc., Hoffman Estates, IL), immediately, 2–6 h and daily for 7–10 d after administration of  $^{131}\text{I}$ -Lym-1. Conjugate anterior and posterior views of the total body, head, chest, abdomen, pelvis and additional tumor sites were acquired.

Blood samples were obtained on multiple occasions after infusion and daily for 7–10 d thereafter. An aliquot of each sample was counted in a calibrated gamma well detector, and the percentage of the injected dose in the blood was calculated, using the patient's body weight to estimate theoretical blood volume (20).

During the course of the imaging study, all urine was collected from each of the patients and all feces were collected from 2 of the patients. Aliquots of urine were quantitated for  $^{131}\text{I}$  using a calibrated gamma well detector, then were multiplied by the measured urine volume to calculate daily  $^{131}\text{I}$  output.  $^{131}\text{I}$  in each daily fecal sample was determined using two opposed, isoresponsive sodium iodide detectors (Picker Nuclear, North Haven, CT) calibrated against appropriate standards for radionuclide, volume and geometry.

### Image Quantification and Pharmacokinetics

The detailed methods for quantitative planar imaging have been described (19–21). Counts in regions of interest (ROIs) were converted to percentage injected dose (%ID) using a reference source with a known amount of  $^{131}\text{I}$ . Using a visual boundary, ROIs for total body, organs and tumors were defined on the image with the best contrast in the imaging sequence. Lungs and kidneys were processed using separate ROIs for each of the pair, and the calculated %ID for each pair was added together. When there was concentration of  $^{131}\text{I}$  in tissues overlaying an organ (e.g., liver overlaying kidney), an aliquot method was used, wherein counts

per pixel were obtained for the organ region without overlap and were adjusted for the total number of pixels in the organ. Background regions were selected in an area of the body with the same thickness as that of the tissue overlaying the organ or tumor to subtract background  $^{131}\text{I}$ . Coincidence correction was required when the  $^{131}\text{I}$  radioactivity in the patient was greater or equal to 1.1 GBq (30 mCi). A correction factor was determined by comparison of counts in a reference source imaged with and without the radioactive patient in the field of view on each imaging occasion (22). The geometric mean method (23,24) was used for image quantification of the total body, liver and spleen, because these tissues were clearly seen from anterior and posterior views. The effective point source method (19) was used to determine the radioactivity in tissues seen on only one of the conjugate views (e.g., kidneys, lumbar vertebrae, thyroid, tumor).

For each organ, radioactivity in the ROI was converted to %ID after attenuation correction; regression fitting of the %ID was performed to obtain biologic half-time and cumulated activity. A monoexponential function was used to obtain biologic half-time for all tissues, including the three lumbar vertebrae (25) and the total body. A cubic spline function was used on a few occasions when a monoexponential fit was not possible (e.g., some tumors). For blood, a biexponential function was used, because it was invariably the best fit.

The volume of each palpable tumor was determined using caliper measurements, and the volume of each nonpalpable tumor was determined using CT or MR images. Tumors located in bone and tumors with mass < 2 g by caliper measurement or < 10 g by CT measurement were excluded from the analyses to ensure accuracy. A total of 120 tumors (99 superficial, 21 deep) in 45 patients met the aforementioned requirements for quantification; 49 tumors in the MTD patients, 52 tumors in the LD NHL patients and 19 tumors in the LD CLL patients. To assess the accuracy of quantification, we obtained biopsy samples from four tumors 1 or 3 d after administration of  $^{131}\text{I}$ -Lym-1. Relatively large specimens (each with mass  $\geq 0.4$  g) were excised to reduce the problem of heterogeneity of  $^{131}\text{I}$  distribution in the tumor.  $^{131}\text{I}$  concentrations (MBq/g) in the samples were measured using a calibrated gamma well detector and were compared with concentrations obtained using gamma camera image quantification.

### Radiation Dosimetry

Medical internal radiation dose (MIRD) methods were used to obtain radiation absorbed doses, taking contributions from all sources, including the remainder in the body, into consideration (26). The MIRD S values and reference man masses (27) were used for all organs except the spleen. Patient-specific splenic dose was determined using spleen volume obtained from CT images (28). Similarly, tumor volumes were obtained using CT and caliper measurements; tumor radiation dose was determined for nonpenetrating  $^{131}\text{I}$  radiation in the tumor and penetrating radiation in the total body.

Radiation dose to the bone marrow was determined using two methods:  $^{131}\text{I}$  penetrating radiation from the total body was added to that of nonpenetrating radiation from the blood to obtain nonspecific components of marrow radiation, as previously reported (20); and  $^{131}\text{I}$  nonpenetrating radiation was obtained by vertebral imaging to obtain the specific component of marrow radiation (29). The calculation of marrow radiation from blood  $^{131}\text{I}$  assumed that the specific activity of the blood in the marrow was

25% that of the blood (20). The calculation of marrow radiation from the total body assumed a uniform distribution of  $^{131}\text{I}$  in the body. S values for penetrating emissions were obtained by subtracting the S values for nonpenetrating emissions from the S values for penetrating and nonpenetrating emissions using MIRD data (20). The specific radiation dose to marrow assumed that the red marrow mass in three lumbar vertebrae, quantified by imaging, constituted 6.7% of total red marrow mass, as reported (29). The extrapolated value for cumulated activity in the total marrow mass and the S value for nonpenetrating  $^{131}\text{I}$  emissions were used to calculate the specific radiation dose to marrow (25).

### Statistical Methods

The arithmetic mean, median, SD and range were calculated for patient characteristics, dosages, clearances and organs by groups as indicated in the text and tables. Where tables include values for "tumor," a mean value among all evaluable tumors for a patient was determined. This mean value was then used in the calculation of summary statistics for the specified patient group.

Comparisons between patient groups (i.e., MTD versus LD or CLL versus NHL) were examined using the nonparametric Wilcoxon rank sum test (30). This test ranks the measure (i.e., organ radiation dose) from smallest to largest and then tests whether the larger ranks tend to belong to one group or the other. Analysis of relationships between two measures (e.g., tumor size versus tumor radiation dose, Gy/GBq) was done using the Spearman rank correlation coefficient (30). For this test, each measure is ranked from smallest to largest. The test is based on determining whether a patient with a higher rank relative to one measure would also tend to have a higher ranking on the other. For both the Wilcoxon and the Spearman tests, the *P* value is an indication of whether the observed rankings are grouped in a way that is unlikely to be the result of chance. Statistical significance was defined as  $P \leq 0.05$ . For a number of these comparisons, individual tumor measurements needed to be compared (e.g., size versus radiation dose, Gy/GBq). Therefore, for hypothesis testing purposes, up to two tumors per patient were identified, the one that received the highest and the one that received the lowest radiation dose. In a few patients, no tumor met the standards for accurate evaluation, and these patients could not be included in the dose comparisons. If tumor dose could only be described for one tumor for a patient, that tumor was defined as both the high-dose and the low-dose tumor. Statistical hypothesis tests were then done twice to address each question, once using the high-dose and once using the low-dose tumor. Because the results were always in concordance, the text simply states that the relationship to the tumor measurement was either statistically significant or not and, if it was, reports the more conservative (larger) of the two *P* values.

## RESULTS

### Pharmacokinetics

Clearance of  $^{131}\text{I}$  from the patient (total body) was monoexponential with a biologic half-time of approximately 36 h (Table 1). Urine clearances correlated reciprocally with body clearances; a mean of 32 %ID was in the urine by 24 h. The accumulated fecal excretion was less than 2 %ID for each of 2 patients for 7 d after  $^{131}\text{I}$ -Lym-1 infusion. Blood clearance of  $^{131}\text{I}$ -Lym-1 was biexponential with fast (alpha) and slow (beta) phases (Table 1), which were similar for all

**TABLE 1**  
Biologic Half-Time for <sup>131</sup>I-Lym-1 Therapy Dose

Site	Maximum tolerated dose NHL (n = 20)	Low dose	
		NHL (n = 26)	CLL (n = 5)
Total body	36 ± 19	34 ± 10	38 ± 10
Blood, alpha	5 ± 4	3 ± 3	1 ± 1
Blood, beta	29 ± 9	34 ± 12	28 ± 11
Liver	19 ± 5	19 ± 12	19 ± 10
Spleen	22 ± 7	22 ± 12	12, 19*
Marrow†	24 ± 10	22 ± 12	24 ± 5
Lung	24 ± 12	24 ± 10	19 ± 5
Kidney	24 ± 7	29 ± 17	26 ± 4
Thyroid	48 ± 22	36 ± 43	43 ± 17
Tumor	43 ± 17	43 ± 31	48 ± 29

\*3 of 5 CLL patients had splenectomy.

†Lumbar marrow imaging.

NHL = non-Hodgkin's lymphoma; CLL = chronic lymphocytic leukemia.

Data given as mean ± SD in hours.

of the groups of patients, although CLL patients had a more rapid fast phase. In the CLL patients, more rapid blood clearance may account for lower radiation doses received by some organs.

Pharmacokinetics as reflected by the biologic half-time (Table 1) and concentration (%ID/g) (Tables 2–4) of <sup>131</sup>I-Lym-1 were similar for patients in the MTD and LD trials. This was also the case for the NHL and CLL patients in the LD trial, except that the CLL group had lower tumor concentration of <sup>131</sup>I (%ID/g). The biologic half-time and concentration of <sup>131</sup>I in tumors was about twice that in normal tissues, except that the biologic half-time of the thyroid was similar to that of tumor. The mean biologic half-time of the body and most normal tissues was one half

to three fourths that of tumor or thyroid and was similar between groups of patients, except the CLL group. Concentration of <sup>131</sup>I in tumors usually reached a maximum at 6–24 h after infusion and decreased thereafter; normal tissues characteristically had peak concentration of <sup>131</sup>I immediately and decreased monoexponentially thereafter. Peak liver concentration of <sup>131</sup>I almost invariably occurred immediately after infusion (Tables 2–4), thereby verifying the adequacy of the Lym-1 to saturate hepatic receptors. Quantification of tumor <sup>131</sup>I by imaging and by counting biopsy samples showed good correlation over a range of tumor <sup>131</sup>I concentrations of  $3 \times 10^{-3}$  to  $9 \times 10^{-5}$  %ID/g. The mean difference between imaging and biopsy data was 18% (range 11%–22%).

#### Radiation Dosimetry

There were no differences in radiation dose (Gy/GBq) to body, tumor, spleen, nonspecific marrow, kidney or thyroid between groups of patients entered on MTD and LD trials ( $P > 0.1$ ; Table 5, Fig. 1). Statistical differences in radiation doses, of no biologic significance, for specific marrow, liver and lung were found between these groups of patients. Biologically important differences were reflected in the differences between NHL and CLL patients in the LD trial, in which the CLL group had lower mean tumor (and blood) and higher mean liver radiation doses (Gy/GBq) but only the liver values were statistically different ( $P = 0.003$ ), probably due to the small number of CLL patients available for analysis.

For all patients in the MTD and LD trials, the mean nonspecific marrow radiation dose was 0.11 Gy/GBq (0.39 rad/mCi) consisting of 0.05 Gy/GBq (0.20 rad/mCi) contributed by the body and 0.05 Gy/GBq (0.19 rad/mCi) by the blood. Although the mean marrow radiation dose, calculated as the sum of penetrating radiation from body and nonpenetrating radiation from blood, was similar to the mean

**TABLE 2**  
Tissue Concentration of <sup>131</sup>I for 20 NHL Patients Entered in Maximum Tolerated Dose Trial

Time postinjection	Liver (1809 g)*	Spleen (140–2077 g)†	Lung (999 g)*	Kidney (284 g)*	Thyroid (20 g)*	Tumor (2–374 g)‡
Immediate (%ID)	17.6 ± 5.6	4.6 ± 1.7	8.3 ± 2.3	2.9 ± 1.5	0.12 ± 0.1	0.6 ± 0.5
Range	9.3–26.3	2.1–8.0	5.8–12.7	1.4–7.0	0.0–0.4	0.1–1.9
Immediate (%ID/g)	0.010 ± 0.003	0.014 ± 0.007	0.008 ± 0.002	0.010 ± 0.005	0.006 ± 0.005	0.024 ± 0.035
Range	0.005–0.015	0.003–0.025	0.006–0.013	0.005–0.025	0.000–0.019	0.001–0.161
Peak (%ID)	17.6 ± 5.6	4.9 ± 1.7	8.3 ± 2.3	3.1 ± 1.5	0.2 ± 0.1	0.7 ± 0.6
Range	9.3–26.3	2.1–8.2	5.8–12.7	1.4–7.0	0.1–0.4	0.1–2.1
Peak (%ID/g)	0.010 ± 0.003	0.015 ± 0.008	0.008 ± 0.002	0.011 ± 0.005	0.009 ± 0.004	0.030 ± 0.035
Range	0.005–0.015	0.003–0.031	0.006–0.013	0.005–0.025	0.004–0.019	0.003–0.162
Time to peak (h)	0 ± 0	2 ± 3	0 ± 0	2 ± 3	4 ± 8	7 ± 6
Range	0–0	0–6	0–0	0–6	0–24	0–24

\*Medical internal radiation dose mass.

†Observed range for patient-specific CT mass (volume).

‡Observed range for patient-specific CT or caliper mass (volume).

NHL = non-Hodgkin's lymphoma; %ID = percentage injected dose.

Tissue concentrations are given as mean ± SD.

**TABLE 3**  
Tissue Concentration of <sup>131</sup>I for 26 NHL Patients Entered in Low-Dose Trial

Time postinjection	Liver (1809 g)*	Spleen (142–1023 g)†	Lung (999 g)*	Kidney (284 g)*	Thyroid (20 g)*	Tumor (2–509 g)‡
Immediate (%ID)	16.2 ± 7.9	5.8 ± 3.1	10.1 ± 3.7	2.4 ± 0.7	0.2 ± 0.0	0.8 ± 1.5
Range	6.7–36.5	2.0–13.1	3.0–15.5	1.8–3.7	0.1–0.2	0.0–7.0
Immediate (%ID/g)	0.009 ± 0.004	0.015 ± 0.008	0.010 ± 0.004	0.008 ± 0.002	0.010 ± 0.002	0.019 ± 0.015
Range	0.004–0.020	0.006–0.034	0.003–0.015	0.006–0.013	0.005–0.016	0.003–0.055
Peak (%ID)	16.3 ± 7.8	6.5 ± 3.4	10.8 ± 3.7	2.7 ± 0.7	0.2 ± 0.0	0.9 ± 1.5
Range	6.7–36.5	2.1–14.2	3.6–15.5	1.8–3.7	0.2–0.4	0.0–7.1
Peak (%ID/g)	0.009 ± 0.004	0.017 ± 0.010	0.011 ± 0.004	0.009 ± 0.003	0.012 ± 0.004	0.021 ± 0.014
Range	0.004–0.020	0.007–0.051	0.004–0.015	0.006–0.013	0.008–0.019	0.003–0.060
Time to peak (h)	0 ± 1	3 ± 5	3 ± 7	2 ± 3	10 ± 10	10 ± 9
Range	0–6	0–24	0–24	0–6	0–24	0–24

\*Medical internal radiation dose mass.

†Observed range for patient-specific CT mass (volume).

‡Observed range for patient-specific CT or caliper mass (volume).

NHL = non-Hodgkin's lymphoma; %ID = percentage injected dose.

Tissue concentrations given as mean ± SD.

marrow radiation dose obtained by lumbar vertebral imaging, the latter marrow doses were more variable among patients than were those obtained by the body and blood method (Fig. 2). If the body and blood contributions were added to the marrow dose obtained by imaging, then the total marrow dose was doubled, reflecting the significance of specific radiation from targeting of marrow lymphoma (29).

Mean tumor radiation dose was about nine times that of the body or marrow for all NHL patients, whether in the MTD or LD trials (Table 5). There was an inverse association between tumor size and radiation dose, with larger tumors receiving less radiation dose ( $P < 0.01$ ). Splenic radiation varied somewhat but was sufficient to decrease splenic size in some patients with splenomegaly (Fig. 3). The mean radiation doses for lung, kidney and thyroid in all

patients assessed were 0.3, 0.3 and 0.6 Gy/GBq (1.2, 1.1 and 2.1 rad/mCi), respectively. The mean tumor dose for all patients was 1.0 Gy/GBq (range 0.1–3.5 Gy/GBq [3.7 rad/mCi, range 0.4–12.9 rad/mCi]).

#### Comparison of Tumor Dosimetry with Patient Parameters

There were no significant relationships between tumor radiation dose (per unit of administered <sup>131</sup>I, Gy/GBq, for the initial therapy dose) and amount of <sup>131</sup>I (GBq) or total Lym-1 (mg) administered. Similarly, there were no relationships between tumor radiation dose and LDH (tumor burden), splenic volume, therapeutic response (Fig. 4) or tumor histologic grade (Fig. 5) or type, although the number of tumors was often small when classified by histologic type.

**TABLE 4**  
Tissue Concentration of <sup>131</sup>I for 5 CLL Patients Entered in Low-Dose Trial

Time postinjection	Liver (1809 g)*	Spleen (248, 2826 g)†	Lung (999 g)*	Kidney (284 g)*	Thyroid (20 g)*	Tumor (4–36 g)‡
Immediate (%ID)	18.3 ± 16.3	4.3, 2.5	12.7 ± 2.5	2.0 ± 1.1	0.1 ± 0.1	0.1 ± 0.0
Range	3.4–46.2		9.6–15.5	1.2–3.6	0.1–0.2	0.0–0.2
Immediate (%ID/g)	0.010 ± 0.009	0.017, 0.009	0.013 ± 0.003	0.007 ± 0.004	0.006 ± 0.003	0.007 ± 0.003
Range	0.002–0.026		0.010–0.016	0.004–0.013	0.004–0.010	0.005–0.011
Peak (%ID)	18.3 ± 16.3	4.3, 2.5	12.7 ± 2.5	2.0 ± 1.1	0.2 ± 0.2	0.2 ± 0.1
Range	3.4–46.2		9.6–15.5	1.2–3.6	0.1–0.5	0.1–0.3
Peak (%ID/g)	0.010 ± 0.009	0.017, 0.009	0.013 ± 0.003	0.007 ± 0.004	0.011 ± 0.008	0.010 ± 0.003
Range	0.002–0.026		0.010–0.016	0.004–0.013	0.004–0.023	0.005–0.014
Time to peak (h)	0 ± 0	0, 0	0 ± 0	1 ± 2	14 ± 12	11 ± 10
Range	0–0		0–0	0–4	3–24	0–24

\*Medical internal radiation dose mass.

†Observed range for patient-specific CT mass (volume); 3 of 5 patients had splenectomy.

‡Observed range for patient-specific CT or caliper mass (volume).

CLL = chronic lymphocytic leukemia; %ID = percentage injected dose.

Tissue concentrations given as mean ± SD.

**TABLE 5**  
Radiation Absorbed Dose from Initial <sup>131</sup>I-Lym-1  
Therapy Dose

Site	Maximum tolerated dose	Low dose	
	NHL (n = 20)	NHL (n = 26)	CLL (n = 5)
Total body	0.12 ± 0.05	0.11 ± 0.03	0.12 ± 0.03
Blood	0.20 ± 0.11	0.23 ± 0.14	0.12 ± 0.03
Liver	0.36 ± 0.08	0.27 ± 0.09	0.50 ± 0.18
Spleen	0.59 ± 0.30	0.58 ± 0.22	0.47, 0.30*
Marrow†	0.11 ± 0.04	0.11 ± 0.04	0.08 ± 0.02
Marrow‡	0.12 ± 0.06	0.09 ± 0.08	0.10 ± 0.04
Lung	0.31 ± 0.14	0.36 ± 0.10	0.39 ± 0.13
Kidney	0.31 ± 0.12	0.29 ± 0.06	0.28 ± 0.08
Thyroid	0.49 ± 0.25	0.70 ± 0.35	0.51 ± 0.32
Tumor	1.12 ± 0.70	1.04 ± 0.68	0.61 ± 0.56

\*3 of 5 patients had splenectomy.

†Nonpenetrating radiation from blood and penetrating radiation from body.

‡Nonpenetrating radiation from concentration of <sup>131</sup>I in marrow for marrow targeting.

NHL = non-Hodgkin's lymphoma; CLL = chronic lymphocytic leukemia.

Dosage given as mean ± SD in Gy/GBq.

## DISCUSSION

NHL is one of the few malignancies that has increased in frequency beyond the increase in population. Consequently, lymphomas and related malignancies, such as CLL, have the fourth greatest economic impact of all malignancies in the U.S. Most NHL and CLL are of B-lymphocytic origin and are incurable with standard therapies. Since initial reports on the therapeutic efficacy of <sup>131</sup>I-Lym-1 for RIT in patients with B-lymphocytic NHL and CLL (3,12), others have made similar observations (13,14). Lym-1 is a mouse IgG2a monoclonal antibody that reacts selectively with malignant

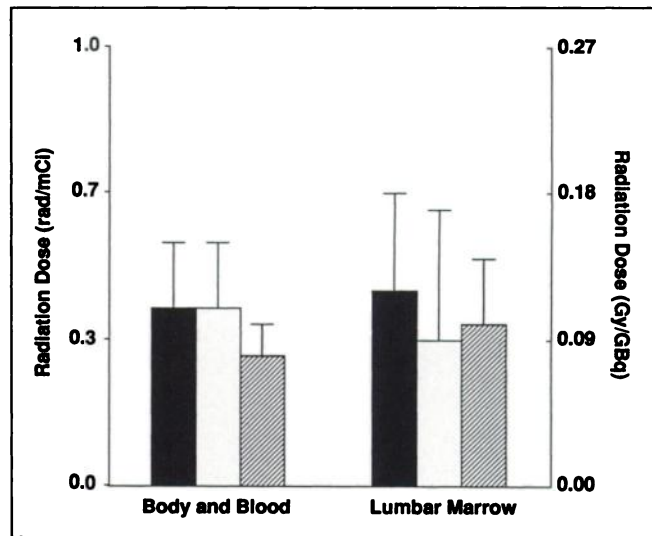
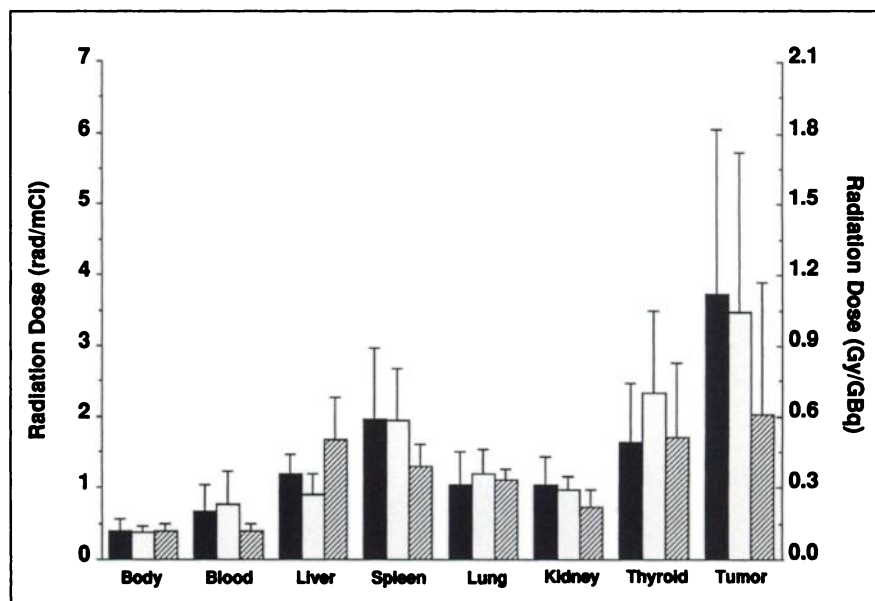


**FIGURE 2.** There were no discerned differences in radiation absorbed doses to marrow by either conventional method (body and blood) or marrow imaging method, when comparing groups of patients entered on MTD (■), LD NHL (□) or CLL (▨) studies. Marrow imaging can add to marrow radiation dose a substantial, variable and specific component, not taken into account by conventional method. Bars represent mean ± SD.

lymphoid cells of B-lymphocyte lineage, does not react with other normal, nonlymphoid tissues and reacts less strongly with subsets of nonmalignant B lymphocytes (18). The pharmacokinetics and radiation dosimetry observed for <sup>131</sup>I-Lym-1 in the patients reported herein are consistent with the tissue immunophenotypic profile reported for Lym-1.

There are two broad approaches to radionuclide dosing schedules for radioimmunotherapy. One of these is the administration of a single, large dose of radiolabeled antibody, most commonly associated with bone marrow transplantation; this approach has been used by Press et al. (5) and, more recently, by Kaminski et al. (6) for NHL.

**FIGURE 1.** There were no discerned differences in radiation absorbed doses to body, liver, spleen, lung, kidney or thyroid between groups of patients entered on MTD (■), LD NHL (□) or CLL (▨) studies; there were minor, but statistically significant, differences when entire LD group was compared with MTD group, as noted in text. Bars represent mean and SD.



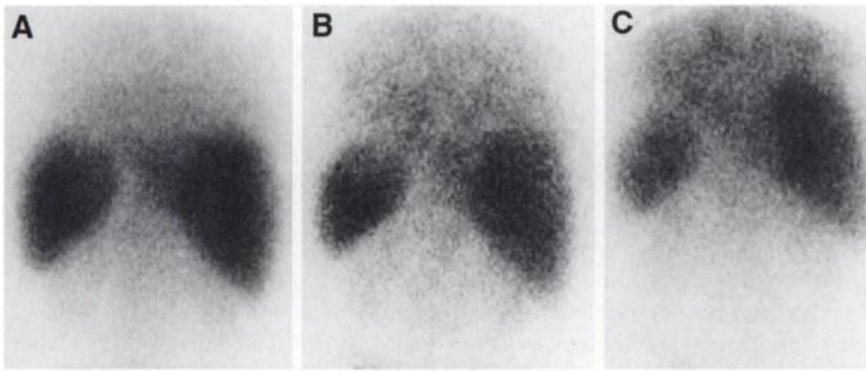


**FIGURE 3.** In some patients with splenomegaly, radiation doses were sufficient to decrease splenic size. Spleen was 968 mL by CT before therapy (A), 592 mL after one dose (6.07 GBq [164 mCi]) (B) and 474 mL after five doses (C) of  $^{131}\text{I}$ -Lym-1 (cumulative 20.6 GBq [558 mCi]). Radiation doses to spleen from first dose and from five doses were 0.89 Gy (89 rad) and 4.70 Gy (470 rad), respectively. Spleen images were obtained immediately after  $^{131}\text{I}$ -Lym-1 administration.

Potential advantages of a single large dose of radionuclide include less repairable sublethal malignant cell damage and avoidance of interruption of therapy because of HAMA. However, antibodies have difficulty penetrating the tumor, because they are macromolecules (31). Nonuniform blood flow, elevated interstitial pressure, necrotic regions and absent antigenic targets on some of the cells contribute to heterogeneous distribution of antibodies (32).  $^{131}\text{I}$ , with beta radiations that traverse 100 or more cell diameters, distributes the radiation more uniformly throughout the tumor. Despite more uniform cytotoxicity provided by radionuclides like  $^{131}\text{I}$ , nonuniform radiation dose to different regions of the tumor continues to be a problem. A common approach to dosing is to divide the total dose of radionuclide into multiple fractions. This approach has proven effective for  $^{131}\text{I}$  treatment of thyroid cancer. The rationale for fractionated RIT is based on evidence that the radiation dose to the tumor and the dose tolerated by normal tissues can be increased (33,34). Another potential advantage of fractionating the total radionuclide dose into multiple doses is better distribution of the microscopic radiation dose because of reduced heterogeneity of antibody targeting over several doses. Using a colon tumor xenograft model that mimics the heterogeneity of antigen and antibody distribution, Schlom

et al. (34) have shown the benefits of fractionated RIT in mice. An otherwise lethal dose of  $^{131}\text{I}$ -labeled immunospecific antibody, when divided into two doses equivalent in total  $^{131}\text{I}$ , reduced or eliminated tumor growth in 90% of mice, and only 10% of the mice died of toxicity. Fractionation into three doses permitted dose escalation by 50% and more therapeutic benefit; similar results have been reported by others (35).

More than one dose of  $^{131}\text{I}$ -Lym-1 was intended for all of our patients. Originally, individual  $^{131}\text{I}$ -Lym-1 doses of 1.1 or 2.2 GBq (30 or 60 mCi) at 2- to 6-wk intervals (LD) were administered. Most patients were remarkably tolerant of this dosing schedule; one patient received 16 doses (1.1–3.85 GBq, total of 38.7 GBq [30–104 mCi, 1046 mCi]) over 23 mo before developing grade 3 thrombocytopenia. Subsequently, the MTD was determined by dose escalation of  $^{131}\text{I}$  in patient cohorts. The MTD of  $^{131}\text{I}$ -Lym-1 was determined to be 3.7 GBq/m<sup>2</sup> (100 mCi/m<sup>2</sup>) for each of the first two doses separated by an interval of 4 wk (4). All of the patients who received the MTD had complete and durable remissions.

There was a remarkable similarity in the pharmacokinetic and radiation dosimetric data, on average, for the patients in the MTD and LD trials, despite differences in histology,  $^{131}\text{I}$

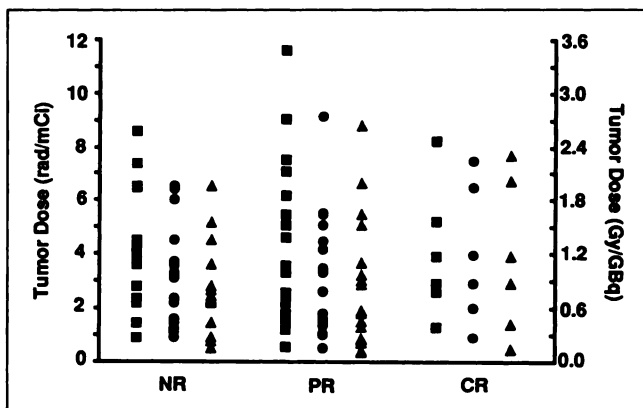


**FIGURE 4.** Maximum (■), mean (●) and minimum (▲) radiation doses (Gy/GBq of administered  $^{131}\text{I}$  for initial therapy dose) for tumors in each patient were compared with therapeutic response. There were no discerned differences. NR = less than partial remission; PR = partial remission; CR = complete remission.

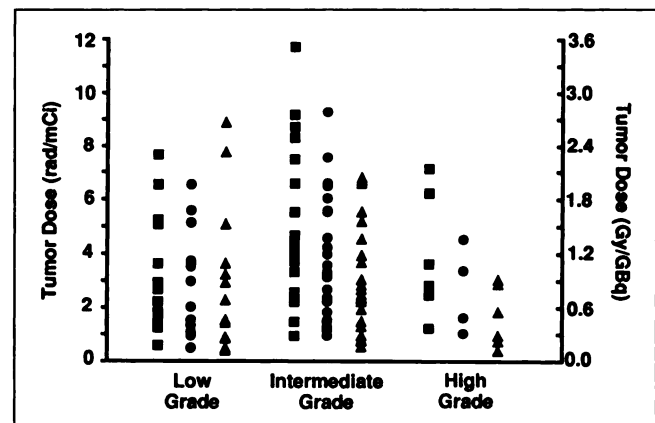


**FIGURE 5.** Maximum (■), mean (●) and minimum (▲) radiation doses (Gy/GBq) for tumors in each patient were compared with histologic grade and type. As illustrated by data for histologic grade, there were no discerned differences, although number of tumors was often small when classified by histologic type.

dose and Lym-1 amount. Additionally, a separate analysis of the entire patient population revealed no evidence for influence of  $^{131}\text{I}$  dose or Lym-1 amount on pharmacokinetic and dosimetric data. This is consistent with previously reported data for Lym-1, wherein tracer doses predicted dosimetry for therapy doses of  $^{131}\text{I}$  in individual patients (16), and with data showing that radioiodinated Lym-1 pharmacokinetics were stable once a threshold of a few milligrams of Lym-1 was exceeded. However, it must be emphasized that myeloablative doses of  $^{131}\text{I}$  were not involved and the amount of Lym-1 was chosen to exceed the minimum amount required for optimal pharmacokinetics. Patients with NHL had similar pharmacokinetics and dosimetry even when analyzed for differences in histologic grade and type. Patients with CLL also had similar pharmacokinetics and dosimetry, except that the  $^{131}\text{I}$  concentration and radiation dose were less for tumor and greater for liver than were those for the patients with NHL.

As expected, tumor concentration of  $^{131}\text{I}$  and radiation dose varied among tumors and among patients. However, the pharmacokinetics and radiation dosimetry of  $^{131}\text{I}$ -Lym-1 for normal tissues were quite similar among patients. Clearance of  $^{131}\text{I}$  from the body was invariably monoexponential with a mean biologic half-time of 36 h. Blood clearance of  $^{131}\text{I}$ -Lym-1 was biexponential with mean biologic half-times of 3.4 and 31.1 h for the fast and slow phases, respectively.  $^{131}\text{I}$ -Lym-1 body and blood clearances were similar to those reported for other monoclonal antibodies of the same mouse isotype (7,11,36). Excretion of  $^{131}\text{I}$  was almost entirely in the urine; <2% was excreted in the feces.

Using the total body radiation dose as a surrogate for marrow radiation dose, Kaminski et al. (36) reported 75 cGy to be dose limiting for nonmyeloablative  $^{131}\text{I}$ -anti-CD20 (B1) RIT. For  $^{131}\text{I}$ -Lym-1, the mean radiation dose to the body for all patients was 0.12 Gy/GBq (0.43 rad/mCi), so that 75 cGy corresponds to 6.3 GBq (174 mCi) or 3.7 GBq/m<sup>2</sup> (102 mCi/m<sup>2</sup>), assuming a body surface area of 1.7 m<sup>2</sup>. Thus, the dose-limiting body radiation for B1 is remarkably similar to our observed MTD of 3.7 GBq/m<sup>2</sup> (100 mCi/m<sup>2</sup>). However, our cohort at 3.7 GBq/m<sup>2</sup> tolerated two doses of this size given at an interval of 4 wk.

Although total-body radiation represents a practical approach to guide  $^{131}\text{I}$  dosing in patients who do have no other confounding factors, it should not be applied indiscriminately. Targeting of marrow malignancy by beta-emitting radiolabeled antibodies can add substantially to the baseline radiation dose to normal marrow cells (25,29). As illustrated in this article, methods have been developed to estimate the magnitude of specific marrow radiation dose (29,37). In 1 patient, marrow targeting contributed five times that from either the body or blood. Using lumbar imaging, marrow radiation doses were quite variable among our patients. Marrow radiation obtained by imaging has been demonstrated to correlate best with observed hematologic toxicity

in NHL patients (29). Although marrow radiation is useful for predicting hematologic toxicity, the microscopic complexity of the marrow should be recognized when interpreting targeted marrow radiation doses.

With the exception of the spleen and tumor, and iodide "processing" tissues like the thyroid, stomach and kidney, the  $^{131}\text{I}$  content of normal tissues was maximum soon after injection followed by clearance of a monoexponential nature. Mean initial liver concentration of  $^{131}\text{I}$  was 16 %ID, considerably less than the 29% reported by Kuzel et al. (13). Although radiation doses for the thyroid were somewhat higher than those for other normal tissues, no clinical or laboratory evidence for hypothyroidism was observed, despite follow-up of several years in many of the patients.

Radiation doses to the spleen were higher than those to other normal tissues except the thyroid, even when adjusted for splenic size. In a number of the patients, the spleen was large enough to make splenic malignancy probable. However, radiation dose to the spleen was about 2.3 times that of normal tissue (lung) even when the spleen was of normal size (<250 mL), which is possible evidence of targeting of malignant or subsets of normal B-lymphocytes (18). Mean splenic radiation dose after correction for splenic volume was about half that for the spleen when uncorrected for volume, thereby emphasizing the importance of patient-specific dosimetry rather than indiscriminate use of "standard man" assumptions. Consistent with observations by Goldenberg et al. (7), who used  $^{131}\text{I}$ -LL2 lymphoma antibody, and in contrast to observations by Press et al. (38), who used B1 antibody, splenomegaly had no evident effect on tumor concentration of, or therapeutic response to,  $^{131}\text{I}$ -Lym-1 (28). Goldenberg et al. observed that tumors could be targeted despite considerable splenic concentration of  $^{131}\text{I}$ -LL2 antibody.

Tumors were visualized in all patients, even in the presence of large tumor burden or marked splenomegaly. Tumors were often well visualized despite the poor imaging characteristics of  $^{131}\text{I}$ . There were no obvious tumors that were missed, although some deep abdominal tumors were poorly visualized. There was no evidence for visualization of normal lymph nodes of Lym-1 negative masses. Because these studies focused on therapy, a rigorous analysis of imaging was not conducted. The mean radiation dose of quantifiable tumors was at least nine times that of marrow and four times that of most normal tissues, but only a little more than twice that of the spleen. Radiation dose to individual tumors, even in the same patients, were highly variable. There was evidence for a relationship between radiation dose and tumor size; tumor concentration of  $^{131}\text{I}$  and radiation dose were significantly higher in smaller tumors. In contrast, there was no evidence for a relationship between tumor radiation dose (per unit of administered  $^{131}\text{I}$ , Gy/GBq, for the initial therapy dose) and tumor therapeutic response or serum LDH, a marker for tumor burden and aggressiveness. Although it was not the purpose of this



study, others have also failed to find a clear dose-response relationship (8).

Based on rigorous phantom and patient studies (22), well-documented coincidence corrections were performed to obtain imaging data. A geometric mean method (23,24) with an attenuation correction factor determined from the  $^{131}\text{I}$  transmission image was used whenever the tissue could be visualized on opposing views. The accuracy and precision of these quantitative imaging methods has been validated in phantoms and in patients (39). Whenever the tissue was not visualized on opposing views, an effective point source method was used with an attenuation coefficient for  $^{131}\text{I}$  in water and a source-to-surface distance obtained from CT. In the case of superficial masses, no attenuation correction was performed, leading to radiation doses to tumors that are probably underestimates. Although few in number, quantification of tumors by gamma well counting of biopsy samples correlated with imaging results.

Radiation dose calculations included nonpenetrating and penetrating  $^{131}\text{I}$  emissions for the target tissue from the target tissue and penetrating  $^{131}\text{I}$  emissions from other visualized tissues and the remaining body. Almost all of the radiation to visualized tissues, including tumors, was due to nonpenetrating  $^{131}\text{I}$  emissions in the target itself, as reported by Shen et al. (40). Although this is not the case for nonvisualized tissues, their radiation doses are likely to be small and to correspond to those of the total body.

## CONCLUSION

Extensive pharmacokinetic and dosimetric data reported herein provide evidence that  $^{131}\text{I}$ -labeled Lym-1 has a favorable therapeutic index that is not readily altered by dose, histologic type or other factors. Additionally, these data for therapy doses are indistinguishable from those reported for tracer doses of  $^{131}\text{I}$ -Lym-1 (16).

## ACKNOWLEDGMENT

This study was supported by National Cancer Institute grant CA47829 and Department of Energy grant DE FG03-84ER60233.

## REFERENCES

1. Armitage JO. Treatment of non-Hodgkin's lymphoma. *N Engl J Med*. 1993;328:1023-1030.
2. Devesa SS, Fears T. Non-Hodgkin's lymphoma time trends: United States and international data. *Cancer Res*. 1992;52:5432s-5440s.
3. DeNardo SJ, DeNardo GL, O'Grady LF, et al. Treatment of a patient with B-cell lymphoma by I-131 Lym-1 monoclonal antibodies. *Int J Biol Markers*. 1987;2:49-53.
4. DeNardo GL, DeNardo SJ, Goldstein DS, et al. Maximum tolerated dose, toxicity, and efficacy of  $^{131}\text{I}$ -Lym-1 antibody for fractionated radioimmunotherapy of non-Hodgkin's lymphoma. *J Clin Oncol*. 1998;16:3246-3256.
5. Press OW, Eary JF, Appelbaum FR, et al. Phase II trial of  $^{131}\text{I}$ -B1 (anti-CD20) antibody therapy with autologous stem cell transplantation for relapsed B-cell lymphomas. *Lancet*. 1995;346:336-340.
6. Kaminski MS, Zasadny KR, Francis IR, et al. Iodine-131-anti-B1 radioimmunotherapy for B-cell lymphoma. *J Clin Oncol*. 1996;14:1974-1981.
7. Goldenberg DM, Horowitz JA, Sharkey RM, et al. Targeting, dosimetry, and radioimmunotherapy of B-cell lymphomas with iodine-131-labeled LL2 monoclonal antibody. *J Clin Oncol*. 1991;9:548-564.
8. Knox SJ, Goris ML, Trisler K, et al. Yttrium-90-labeled anti-CD20 monoclonal antibody therapy of recurrent B-cell lymphoma. *Clin Cancer Res*. 1996;2:457-470.
9. DeNardo GL, DeNardo SJ, Lamborn KR, et al. Low-dose fractionated radioimmunotherapy for B-cell malignancies using  $^{131}\text{I}$ -Lym-1 antibody. *Cancer Biother Radiopharm*. 1998;13:239-254.
10. Vriesendorp HM, Herpst JM, Germack MA, et al. Phase I-II studies of yttrium-labeled antiferritin treatment for end-stage Hodgkin's disease, including radiation therapy oncology group 87-01. *J Clin Oncol*. 1991;9:918-928.
11. Scheinberg DA, Lovett D, Divgi CR, et al. A phase I trial of monoclonal antibody M195 in acute myelogenous leukemia: specific bone marrow targeting and internalization of radionuclide. *J Clin Oncol*. 1991;9:478-490.
12. DeNardo GL, Lewis JP, DeNardo SJ, O'Grady LF. Effect of Lym-1 radioimmunocombinate on refractory chronic lymphocytic leukemia. *Cancer*. 1994;73:1425-1432.
13. Kuzel T, Rosen ST, Zimmer AM, et al. A phase I escalating-dose safety, dosimetry and efficacy study of radiolabeled monoclonal antibody Lym-1. *Cancer Biother*. 1993;8:3-16.
14. Meredith R, Khazaeli MB, Plott G, et al. Comparison of diagnostic and therapeutic doses of  $^{131}\text{I}$ -Lym-1 in patients with non-Hodgkin's lymphoma. *Antibody Immunocnj Radiopharm*. 1993;6:1-11.
15. Non-Hodgkin's Lymphoma Pathologic Classification Project. National Cancer Institute sponsored study of classifications of non-Hodgkin's lymphomas: summary and description of a working formulation for clinical usage. *Cancer*. 1982;49:2112-2135.
16. DeNardo DA, DeNardo GL, Yuan A, et al. Prediction of radiation doses from therapy using tracer studies with iodine-131 labeled antibodies. *J Nucl Med*. 1996;37:1970-1975.
17. Rose LM, Gunasekera AH, DeNardo SJ, DeNardo GL, Meares CF. Lymphoma-selective antibody Lym-1 recognizes a discontinuous epitope on the light chain of HLA-DR10. *Cancer Immunol Immunother*. 1996;43:26-30.
18. Epstein AL, Marder RJ, Winter JN, et al. Two new monoclonal antibodies, Lym-1 and Lym-2, reactive with human-B-lymphocytes and derived tumors, with immunodiagnostic and immunotherapeutic potential. *Cancer Res*. 1987;47:830-840.
19. DeNardo GL, DeNardo SJ, Macey DJ, et al. Quantitative pharmacokinetics of radiolabeled monoclonal antibodies for imaging and therapy in patients. In: Srivastava SC, ed. *Radiolabeled Monoclonal Antibodies for Imaging and Therapy*. New York, NY: Plenum; 1988:293-310.
20. De Nardo GL, Mahe MA, DeNardo SJ, et al. Body and blood clearance and marrow radiation dose of  $^{131}\text{I}$ -Lym-1 in patients with B-cell malignancies. *Nucl Med Commun*. 1993;14:587-595.
21. Erwin WD, Groch MW, Macey DJ, DeNardo GL, DeNardo SJ, Shen S. A radioimmunotherapy and MIRD dosimetry treatment planning program for radioimmunotherapy. *Nucl Med Biol*. 1996;23:525-532.
22. Sorenson JA. Methods of correcting Anger camera deadtime losses. *J Nucl Med*. 1976;17:127-141.
23. Thomas SR, Maxon HR, Kereiakes JG. In vivo quantitation of lesion radioactivity using external counting methods. *Med Phys*. 1976;3:253-255.
24. Eary JF, Appelbaum FL, Durack L, Brown P. Preliminary validation of the opposing view method for quantitative gamma camera imaging. *Med Phys*. 1989;16:382-387.
25. Macey DJ, DeNardo SJ, DeNardo GL, DeNardo DA, Shen S. Estimation of radiation absorbed doses to the red marrow in radioimmunotherapy. *Clin Nucl Med*. 1995;20:117-125.
26. Loevinger R, Berman M. *A Revised Schema for Calculating the Absorbed Dose from Biologically Distributed Radionuclides*. Medical Internal Radiation Dose Pamphlet No. 1. New York, NY: Society of Nuclear Medicine; 1976:1-10.
27. Snyder WS, Ford MR, Warner GG. "S" *Absorbed Dose per Unit Cumulated Activity for Selected Radionuclides and Organs*. Medical Internal Radiation Dose Pamphlet No. 11. New York, NY: Society of Nuclear Medicine; 1975:82-83.
28. Shen S, DeNardo GL, O'Donnell RT, Yuan A, DeNardo DA, DeNardo SJ. Impact of splenomegaly on therapeutic response and I-131-LYM-1 dosimetry in patients with B-lymphocytic malignancies. *Cancer*. 1997;80(suppl):2553-2558.
29. Lim S-M, DeNardo GL, DeNardo DA, et al. Prediction of myelotoxicity using radiation doses to marrow from body, blood and marrow sources. *J Nucl Med*. 1997;38:1374-1378.
30. Hollander M, Wolfe DA. *Nonparametric Statistical Methods*. New York, NY: Wiley; 1973:120.
31. DeNardo GL, DeNardo SJ. Perspectives on the future of radioimmunodiagnosis and radioimmunotherapy of cancer. In: Burchiel SW, Rhodes BA, eds. *Radioim-*

- munoimaging and Radioimmunotherapy*. New York, NY: Elsevier Science; 1983:41–62.
32. Jain RK. Barriers to drug delivery in solid tumors. *Sci Am*. 1994;271:58–65.
  33. Meredith RF, Khazaeli MB, Liu T, et al. Dose fractionation of radiolabeled antibodies in patients with metastatic colon cancer. *J Nucl Med*. 1992;33:1648–1653.
  34. Schlom J, Molinolo A, Simpson JF, et al. Advantage of dose fractionation in monoclonal antibody-targeted radioimmunotherapy. *J Natl Cancer Inst*. 1990;82:763–771.
  35. Buchsbaum DJ, Khazaeli MB, Liu TP, Bright S. Fractionated radioimmunotherapy of human colon carcinoma xenografts with I-131-labeled monoclonal antibody CC49. *Cancer Res*. 1995;55(suppl):5881–5887.
  36. Kaminski MS, Zasadny KR, Francis IR, et al. Radioimmunotherapy of B-cell lymphoma with [<sup>131</sup>I] anti-B1 (anti-CD20) antibody. *N Engl J Med*. 1993;329:459–465.
  37. Siegel JA, Lee RE, Pawlyk DA, Horowitz JA, Sharkey RM, Goldenberg DM. Sacral scintigraphy for bone marrow dosimetry in radioimmunotherapy. *Int J Rad Appl Instrum [B]*. 1989;16:553–559.
  38. Press OW, Eary JF, Appelbaum FR, et al. Radiolabeled-antibody therapy of B-cell lymphoma with autologous bone marrow support. *N Engl J Med*. 1993;329:1219–1224.
  39. Shen S, DeNardo GL, DeNardo SJ, Yuan A, DeNardo DA, Lamborn KR. Reproducibility of operator processing for radiation dosimetry. *Nucl Med Biol*. 1997;24:77–83.
  40. Shen S, DeNardo GL, Macey DJ, et al. Practical determination of organ S values for individual patients for therapy. *Nucl Med Biol*. 1997;24:447–449.